Supporting Information

Alkaline Phosphatase-Mimicking Peptide Nanofibers for Osteogenic Differentiation

ABBREVIATIONS

ALP : Alkaline phosphatase	**OM** : Osteogenic medium
β-gly : β-glycerophosphate	**Osp**: Osteopontin
CaP : Calcium Phosphate	**PCR:** Polymerase chain reaction
CD : Circular dichroism	**pPA** : Phosphatase-like peptide nanostructures
Col-I : Collagen type I	**Pi** : Inorganic phosphate
DFT : Density Functional Theory	**pNPP** : *p*-nitrophenyl phosphate
DMP1 : Dentin matrix protein -1	**PPi** : Pyrophosphate
ECM : Extracellular matrix	**Runx2** : Runt related transcription factor-2
EDX : Energy-dispersive X-ray spectroscopy	**SEM** : Scanning electron microscopy
FBS : Fetal bovine serum	**TEM** : Transmission electron microscopy
Fmoc : Fluorenylmethoxycarbonyl	**XRD** : X-ray diffraction
LC-MS : Liquid chromatography-mass spectroscopy	**MBHA** : methylbenzhydrylamine
MSCs : Mesenchymal stem cells	

Maintenance Media	Normal Media	Osteogenic Media
1. Dulbecco's Modified Eagle Serum (DMEM) 2. 10% Fetal Bovine Serum (FBS) 3. 1% penicillin/streptomycin 4. 2 mM L-glutamine	1. DMEM 2. 10% FBS 3. 1% P/S 4. 2 mM L-glutamine 5. 10mM β-gly	1. DMEM 2. 10% FBS 3. 1% P/S 4. 2 mM L-glutamine 5. 10mM β-gly 6. 0.2 mM Ascorbic Acid 7. 100 nM Dexamethasone

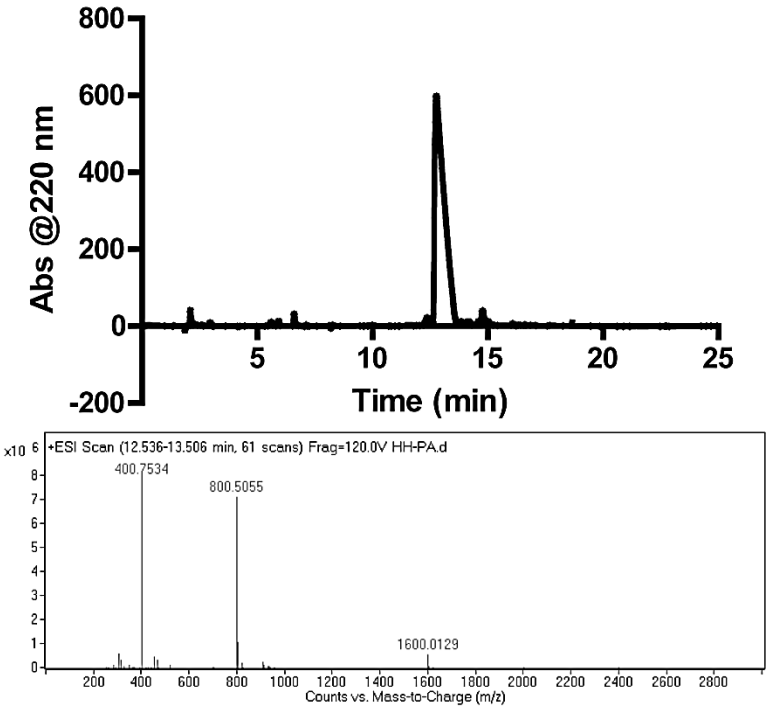

Figure S1. Liquid chromatography and mass spectroscopy results of the pPA molecule. Mass spectrum of peptide after subtracting mass spectrum of water sample. $[M+H]^+$ (calculated) = 800.00, $[M+H]^+$ (observed) = 800.50, $[M/2+H]^+$ (calculated) = 400.00, $[M/2+H]^+$ (observed) = 400.75, $[2M+H]^+$ (calculated) = 1600.00, $[2M+H]^+$ (observed) = 1600.01.

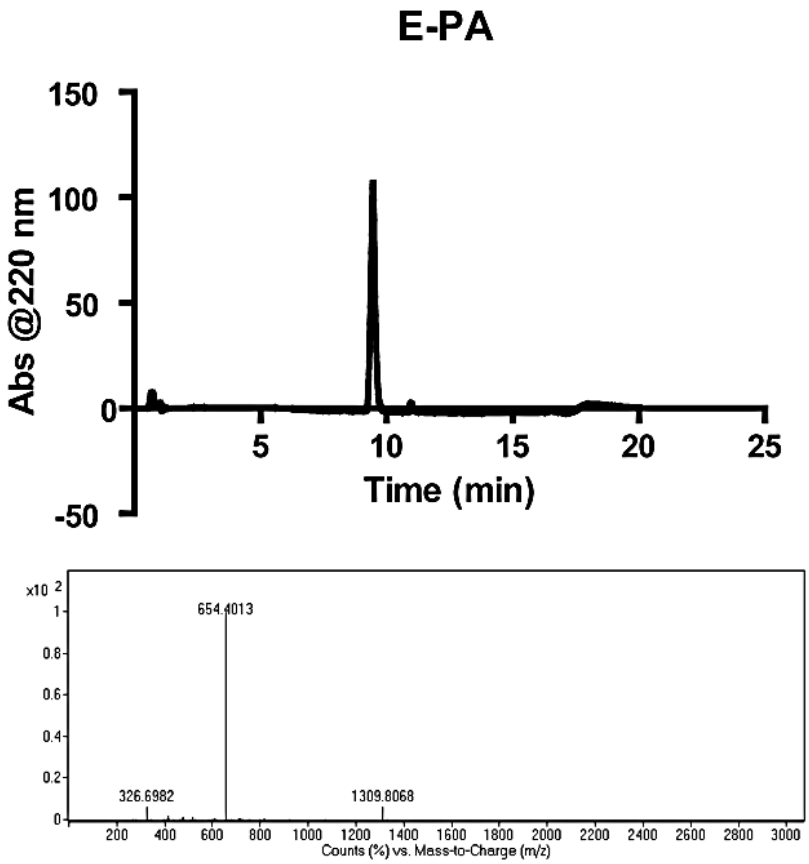

Figure S2. Liquid chromatography and mass spectroscopy results of the E-PA molecule. Mass spectra of peptides after subtracting mass spectra of water samples. For E-PA $[M-H]^-$ (calculated) = 654.82, $[M-H]^-$ (observed) = 654.40, $[2M-2H]^-$ (calculated) = 1309.64, $[2M-2H]^-$ (observed) = 1309.8064, $[M/2-H]^-$ (calculated) = 326.70, $[M/2-H]^-$ (observed) = 326.70.

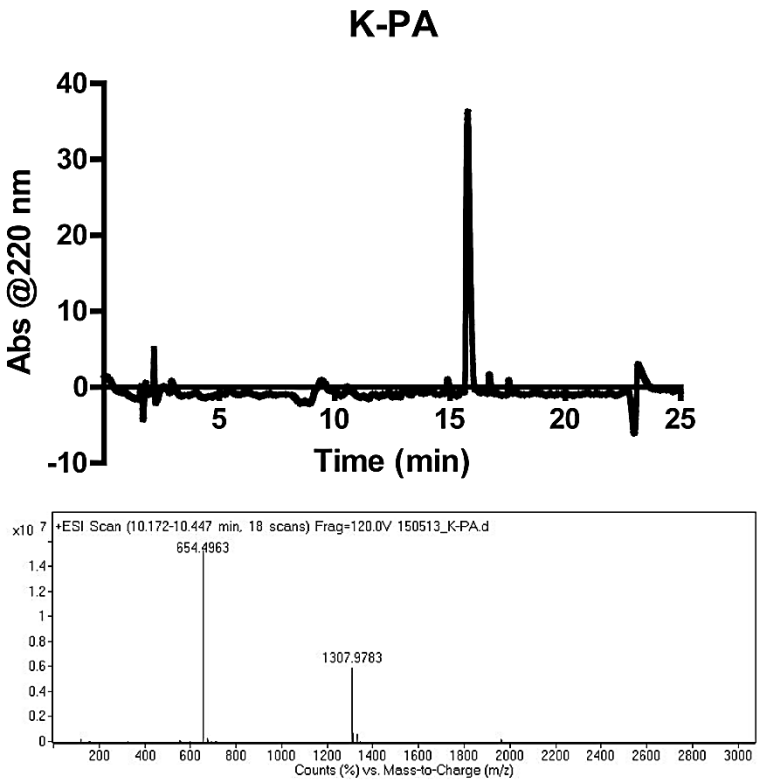

Figure S3. Liquid chromatography and mass spectroscopy results of the K-PA molecule. Mass spectra of peptides after subtracting mass spectra of water samples. For K-PA $[M+H]^+$ (calculated) = 654.90, $[M+H]^+$ (observed) = 654.50, $[2M+H]^+$ (calculated) = 1308.80, $[2M+H]^+$ (observed) = 1307.98.

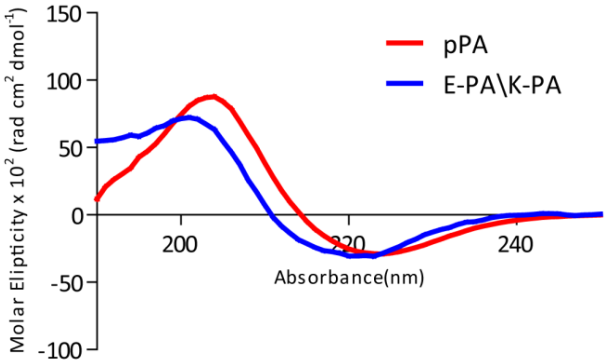

Figure S4. Circular dichroism spectroscopy results of pPA, E-PA\K-PA fiber solution, collected after three reading (3 runs).

	k_{cat} x 10^{-5} (s^{-1})	K_M x 10^{-2} (mM)	k_{cat}/K_m x 10^{-3} (M^{-1} s^{-1})
pPA	1.83 ± 0.13	2.62 ± 1.55	0.69 ± 0.09

	k_{obs} x 10^{-7} (s^{-1})
Imidazole	7.54± 0.36
E-PA\K-PA	6.87± 1.31
Auto Hydrolysis	5.75 ± 0.95

Figure S5. Michaelis-Menten fitting calculations of the phosphatase activity of peptide nanofibers at pH 8.

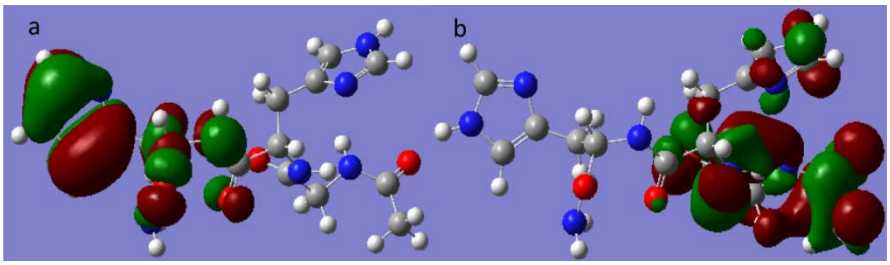

Figure S6. a) HOMO plot of the active sites of pPA and b) LUMO plot of the active site of pPA at the DFT\B3LYP\6-31G (b)\SP level of calculation.

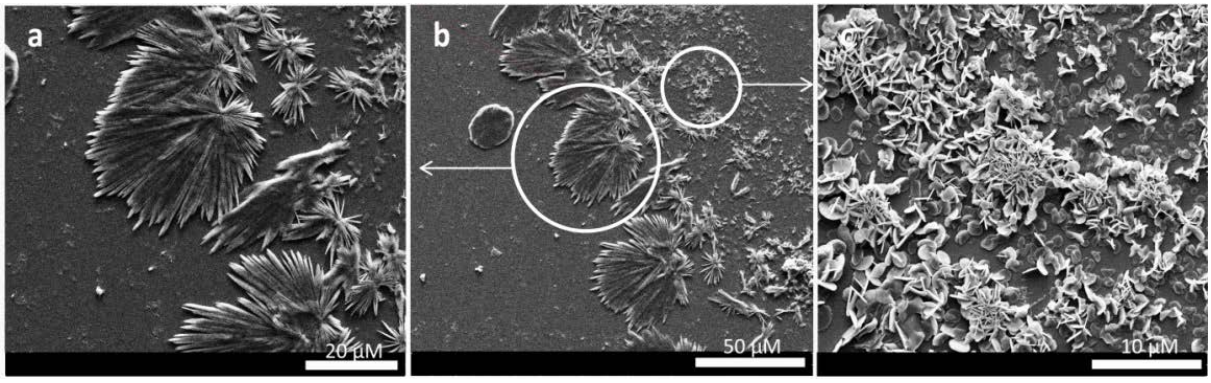

Figure S7. SEM images of mineralization on a, b, c) pPA surfaces at day 3.

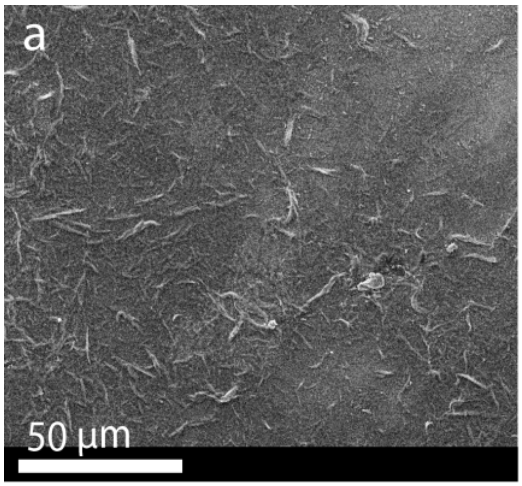

Figure S8. SEM images of CaP deposition on E-PA\K-PA coated surface at day 3. Only the peptide structures were observed.

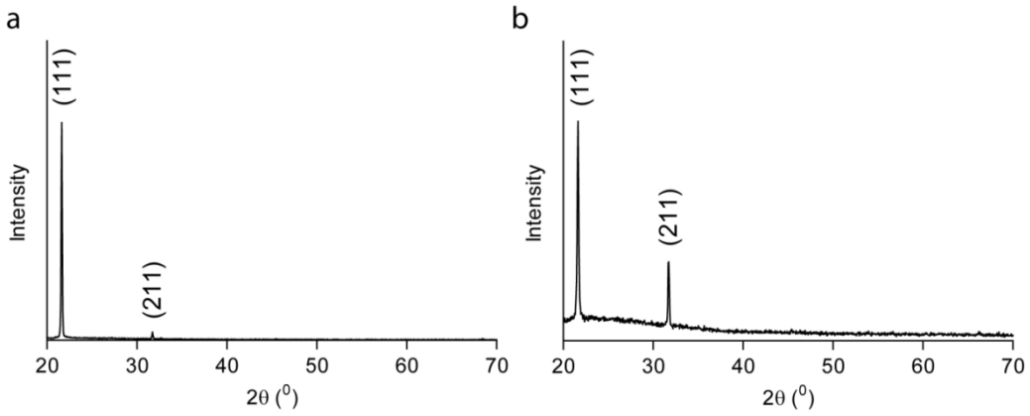

Figure S9. XRD patterns of pPA, a) at day 1, b) at day 3. X-ray diffraction (XRD) patterns of the CaP crystalline phases on peptide coatings correlated to the miller (hkl) indices (200) and (211) of hydroxyapatite (JSPDS card no 73-0293).

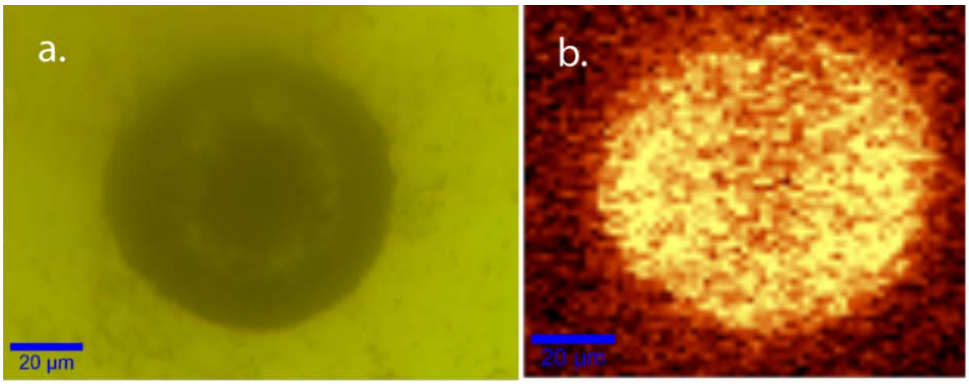

Figure S10. a) Optical (20X) and b) Confocal Raman images of calcium phosphate crystals on pPA coated surfaces.

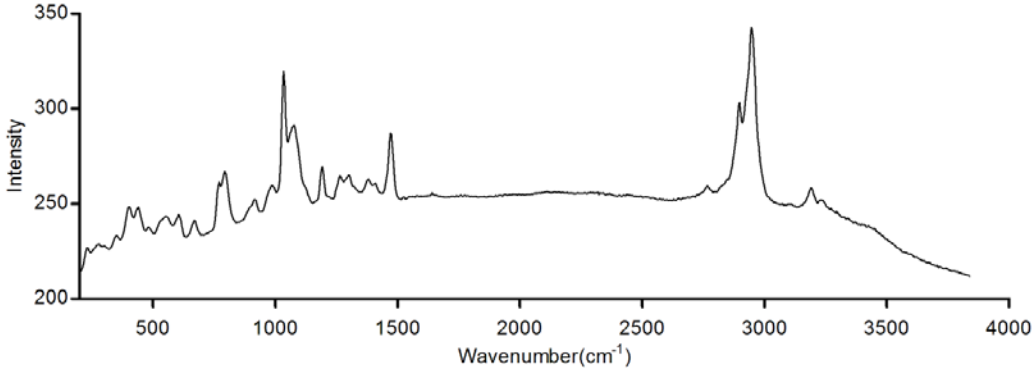

Figure S11. Average Raman spectrum of calcium phosphate crystals formed on a 150 x 150 µm^2 surface of pPA. ν2 = Doubly degenerate bending mode of the PO_4 group (O-P-O bond) (403, 442, 484 cm^{-1}) ν3 = Triply degenerate asymmetric stretching mode of the PO_4 group (P-O bond) (1035, 1076 cm^{-1}) ν4 = Triply degenerate bending mode of the PO_4 group (O-P-O bond) (607 cm^{-1}).

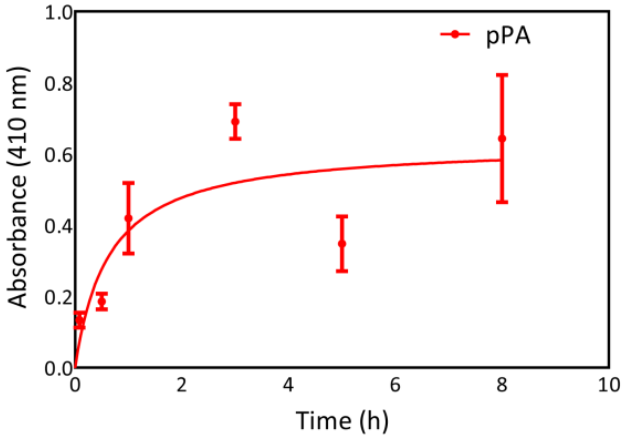

Figure S12. The pNPA hydrolysis activity of pPA coated surfaces, measured through the absorption band of the released pNP at 410 nm.

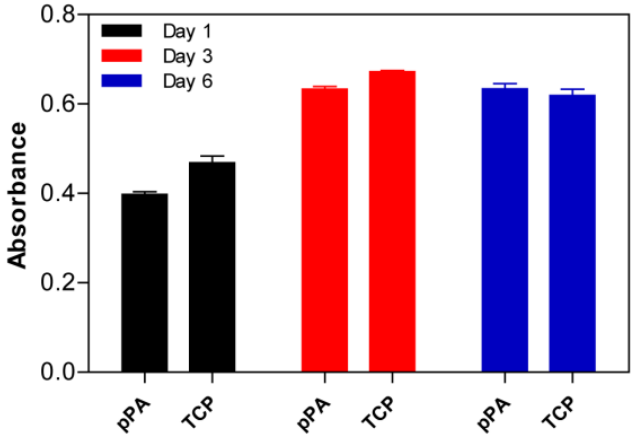

Figure S13. Alamar blue assay for the evaluation of SaOS-2 cell viability on pPA coatings (Mean ± SEM, n = 3).

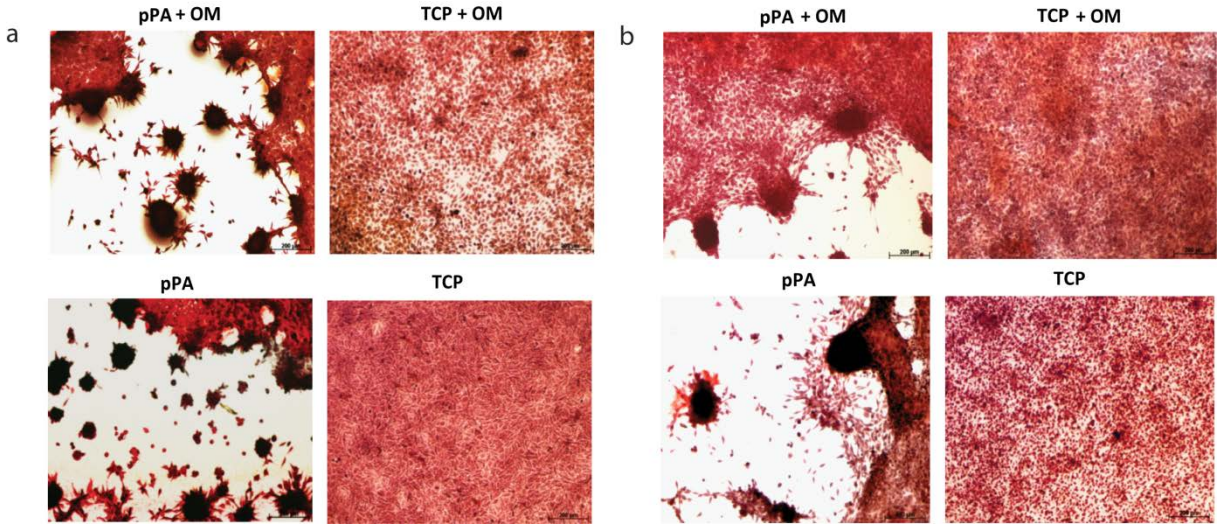

Figure S14. Microscopic images of Alizarin Red S staining results of SaOS-2 cells at a) day 3 and b) day 6, with osteogenic medium (+ OM) and with normal culture medium.

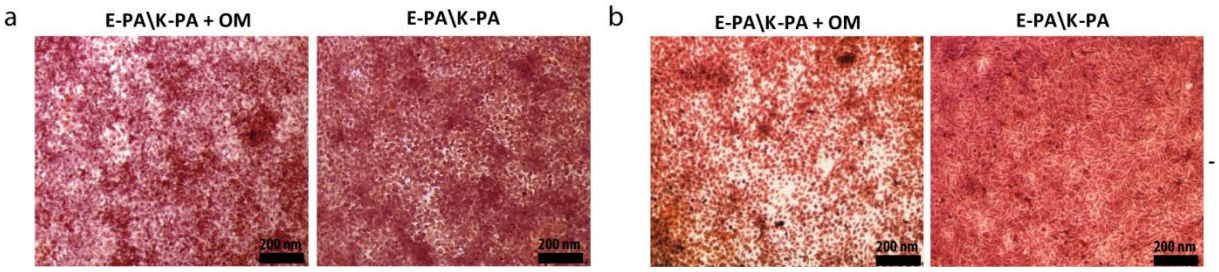

Figure S15. Alizarin Red S staining results of SaOS-2 cells on control groups E-PA\K-PA at a) day 3 and b) day 6, with osteogenic medium (OM) and with normal culture medium.

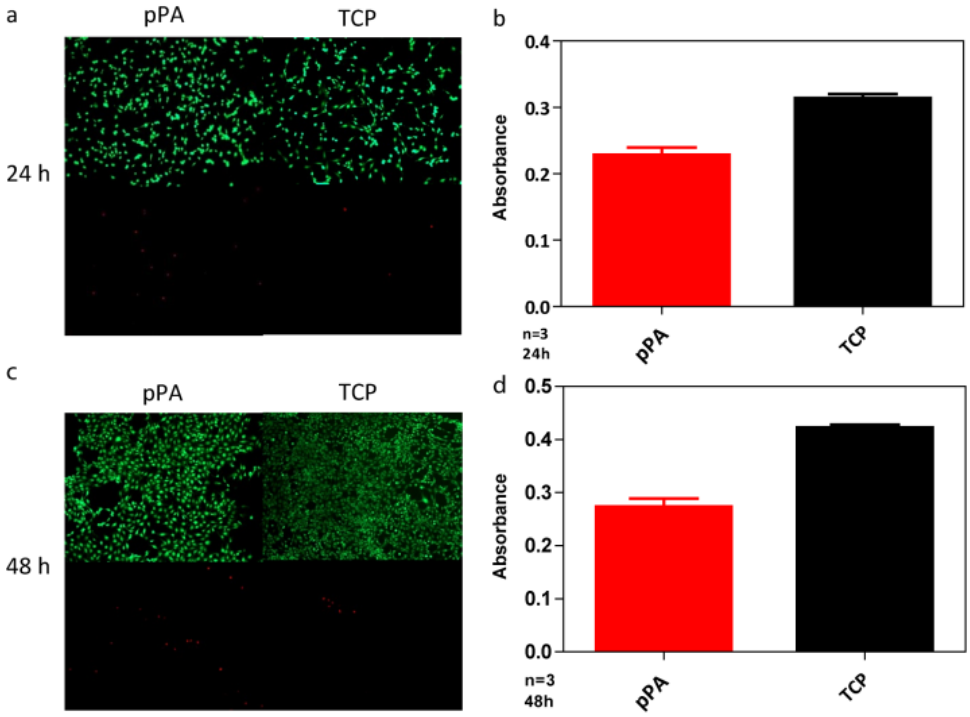

Figure S16. Viability analysis of rMSCs cultured on pPA coatings and tissue culture plate. a, c) Representative Calcein Am (Live=green) and ethidium homodimer (Red=dead) staining and b, d) Alamar Blue assay results for viability. (n = 3).

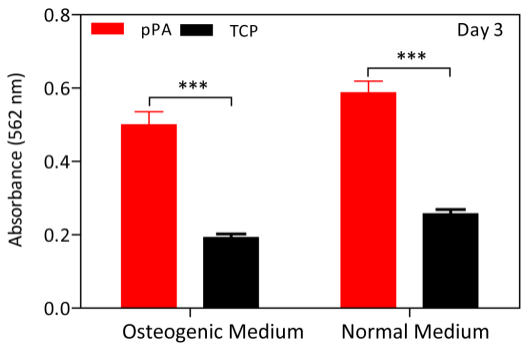

Figure S17. Quantitative analysis of calcium deposition on rMSC cultured surface at day 3. Mean ± SEM, n=4 coatings per sample, one-way analysis of variance (ANOVA) *P < 0.05, **P < 0.01, ***P < 0.0001.

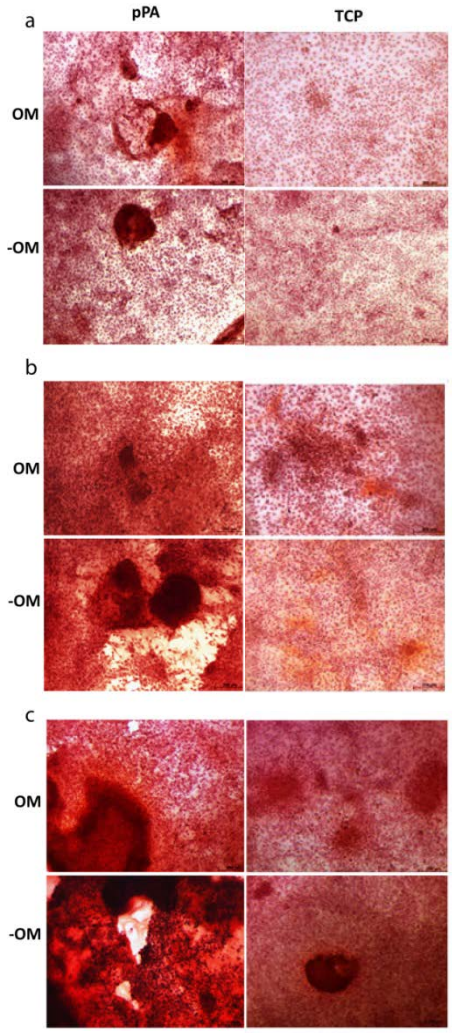

Figure S18. Microscopic images of Alizarin Red S staining results of rMSCs at a) day 3, b) day 7 and c) day 12, with osteogenic medium (OM) and with normal culture medium (-OM).

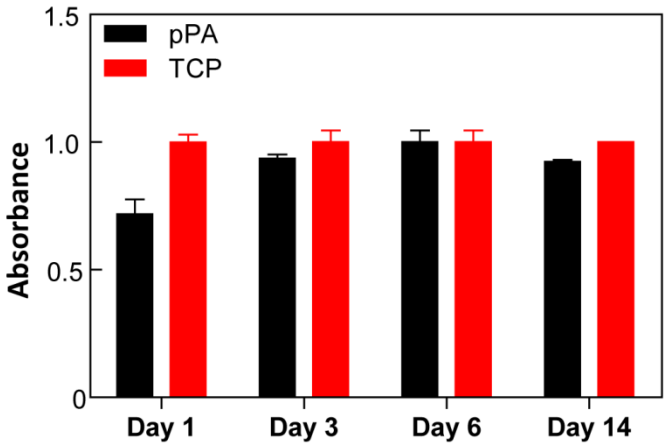

Figure S19. Alamar blue assay for the viability of 3D cell culture of SaOS-2 cells at different time points for understanding the short and long term viability of cells in a 3D peptide scaffold environment (Mean ± SEM, n = 3).

Graph Sketching. Bar charts were sketched and evaluated with Graphpad and images were prepared using Adobe Illustrator.

The program packages Gaussian 09[1] and GaussView[2] were used for theoretical calculations and input and visualization, respectively.

1. Frisch, M. J.; Trucks, G. W.; Schlegel, H. B.; Scuseria, G. E.; Robb, M. A.; Cheeseman, J. R.; Scalmani, G.; Barone, V.; Mennucci, B.; Petersson, G. A.; Nakatsuji, H.; Caricato, M.; Li, X.; Hratchian, H. P.; Izmaylov, A. F.; Bloino, J.; Zheng, G.; Sonnenberg, J. L.; Hada, M.; Ehara, M.; Toyota, K.; Fukuda, R.; Hasegawa, J.; Ishida, M.; Nakajima, T.; Honda, Y.; Kitao, O.; Nakai, H.; Vreven, T.; Montgomery, J. A., Jr.; Peralta, J. E.; Ogliaro, F.; Bearpark, M.; Heyd, J. J.; Brothers, E.; Kudin, K. N.; Staroverov, V. N.; Kobayashi, R.; Normand, J.; Raghavachari, K.; Rendell, A.; Burant, J. C.; Iyengar, S. S.; Tomasi, J.; Cossi, M.; Rega, N.; Millam, J. M.; Klene, M.; Knox, J. E.; Cross, J. B.; Bakken, V.; Adamo, C.; Jaramillo, J.; Gomperts, R.; Stratmann, R. E.; Yazyev, O.; Austin, A. J.; Cammi, R.; Pomelli, C.; Ochterski, J. W.; Martin, R. L.; Morokuma, K.; Zakrzewski, V. G.; Voth, G. A.; Salvador, P.; Dannenberg, J. J.; Dapprich, S.; Daniels, A. D.; Farkas, Ö.; Foresman, J. B.; Ortiz, J. V.; Cioslowski, J.; Fox, D. J. Gaussian, Inc., Wallingford CT, 2009.
2. GaussView, Version 5, Dennington, Roy; Keith, Todd; Millam, John. *Semichem Inc.*, Shawnee Mission, KS, 2009.